C 60 as an Efficient N-Type Compact Layer in Perovskite Solar Cells

ARTICLE *in* JOURNAL OF PHYSICAL CHEMISTRY LETTERS · MAY 2015

Impact Factor: 7.46 · DOI: 10.1021/acs.jpclett.5b00902

10 AUTHORS, INCLUDING:

Konrad Wojciechowski
University of Oxford
15 PUBLICATIONS **682** CITATIONS
SEE PROFILE

Christoph Schlueter
Diamond Light Source
13 PUBLICATIONS **57** CITATIONS
SEE PROFILE

Maximilian Hoerantner
University of Oxford
6 PUBLICATIONS **64** CITATIONS
SEE PROFILE

Jacob Wang
Academia Sinica
12 PUBLICATIONS **1,171** CITATIONS
SEE PROFILE

THE JOURNAL OF PHYSICAL CHEMISTRY Letters

Letter

pubs.acs.org/JPCL

C_{60} as an Efficient n-Type Compact Layer in Perovskite Solar Cells

Konrad Wojciechowski,[†] Tomas Leijtens,[†,‡] Svetlana Siprova,[†,§] Christoph Schlueter,[∥] Maximilian T. Hörantner,[†] Jacob Tse-Wei Wang,[†] Chang-Zhi Li,[⊥] Alex K.-Y. Jen,[⊥] Tien-Lin Lee,[∥] and Henry J. Snaith*[,†]

[†]Clarendon Laboratory, University of Oxford, Parks Road, Oxford, OX1 3PU, United Kingdom

[‡]Center for Nano Science and Technology@Polimi, Istituto Italiano di Tecnologia, via Giovanni Pascoli 70/3, 20133, Milan, Italy

[§]Dipartimento di Fisica, Università della Calabria, via Bucci, Rende, 87036, Italy

[∥]Diamond Light Source Ltd, Harwell Science & Innovation Campus, Didcot, OX11 0DE, United Kingdom

[⊥]Department of Materials Science & Engineering, University of Washington, Seattle, Washington 98195, United States

Supporting Information

ABSTRACT: Organic−inorganic halide perovskite solar cells have rapidly evolved over the last 3 years. There are still a number of issues and open questions related to the perovskite material, such as the phenomenon of anomalous hysteresis in current−voltage characteristics and long-term stability of the devices. In this work, we focus on the electron selective contact in the perovskite solar cells and physical processes occurring at that heterojunction. We developed efficient devices by replacing the commonly employed TiO_2 compact layer with fullerene C_{60} in a regular n−i−p architecture. Detailed spectroscopic characterization allows us to present further insight into the nature of photocurrent hysteresis and charge extraction limitations arising at the n-type contact in a standard device. Furthermore, we show preliminary stability data of perovskite solar cells under working conditions, suggesting that an n-type organic charge collection layer can increase the long-term performance.

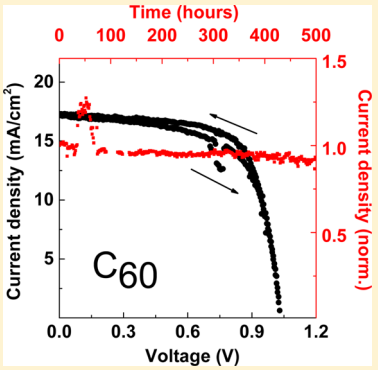

Organic−inorganic lead halide perovskites have been proven to be excellent materials for photovoltaic applications with certified power conversion efficiency (PCE) exceeding 20%.[1] Over the last three years, research into these materials has exploded, which places perovskites as the fastest growing photovoltaic research area with tangible commercial prospects in the near term.[2−8] Application for these materials extends into light emitting devices,[9−11] lasers,[12−14] and photodetectors.[15,16] Such rapid developments and breakthroughs in enhancing efficiency in the solar cells were for a large part achieved by enhancing the crystalline nature of the perovskite films and with suitable interface designing and engineering in a n−i−p solar cell architecture.[5,17−22] The interfaces between the charge selective contacts and the perovskite itself can thus be seen as crucial parameters to explore in attempts to further improve device performance. One pertinent issue for perovskite solar cells is hysteretic behavior commonly occurring during current−voltage characterization. Current output measured during sweeping voltage bias across the terminals of the device is dependent on the direction and speed of scanning, which questions the reliability of extracted photovoltaic performance.[20,23−25] The magnitude of that phenomenon varies between different architectures. Numbers of possible origins have been suggested, including ferroelectric properties of perovskite material,[23,25,26] interface trap states[20,23] or ionic displacement.[23,24,27]

We recently showed that via careful interface engineering, the contact between perovskite and charge extraction layers can be largely improved and hysteretic behavior significantly reduced. By modifying compact TiO_2 with a self-assembled fullerene monolayer, we increased the efficacy of photogenerated charge extraction.[20] We have also recently demonstrated that the hysteretic effect appears to be caused by a long-lived polarization, temporarily changing the electric field profile and charge accumulation within the device to favor charge extraction at the contacts.[28]

Here, we present perovskite solar cells with an n-type selective contact based on a solution-processed fullerene compact layer, entirely removing the compact TiO_2 metal oxide layer as an electroactive component from the device architecture. The use of organic layers facilitates fabricating the entire solar cell at low temperatures (no need for the high-temperature sintering step required to obtain highly crystalline metal oxide layers), suitable for processing involving temperature sensitive substrates, including plastic foil and silicon solar cells. Furthermore, we show that replacing TiO_2 with an organic semiconductor improves charge extraction, influences hysteretic behavior of those cells, and has a large positive impact on steady-state efficiency at the maximum power point.

Received: May 1, 2015
Accepted: May 28, 2015

DOI: 10.1021/acs.jpclett.5b00902
J. Phys. Chem. Lett. 2015, 6, 2399−2405

We employ hard X-ray photoelectron spectroscopy (XPS) to determine the band alignment across the different layers to show how the organic contact facilitates an improved band alignment for charge extraction. Using steady-state and time-resolved photoluminescence spectroscopy on working devices, we shed more light on the mechanistic origin of the hysteresis phenomenon, linking it to electron extraction. Lastly, we present an initial data set of stressing encapsulated perovskite solar cells under simulated full sunlight at 60 °C under load for 500 h and observe that devices incorporating the C_{60} charge selective layers preserve the photocurrent significantly better than the cells with TiO_2 compact layers.

We applied solution-processed fullerene (C_{60}) films, spin-coated from dichlorobenzene solution, as an electron selective compact layer, directly on top of FTO-coated glass substrates (TEC15). In Supporting Information Figure S1 we present SEM and AFM images of C_{60} layers on FTO glass, showing good coverage and uniformity of the fullerene compact films.

In order to investigate the nature of the C_{60}/perovskite contact and the ability of the organic layer to extract electrons, we performed time-resolved photoluminescence (PL) measurements of perovskite films with and without a C_{60} layer (Figure S2). PL is quenched more efficiently with C_{60} molecules than TiO_2, which is revealed by significantly faster PL decay. Since electron diffusion within the perovskite is expected to be similar in both cases, the result indicates a difference in the electron transfer efficiency at the perovskite/quencher interface, suggesting a greatly improved electronic coupling between the perovskite and fullerene as compared to the perovskite and TiO_2.

To gain insight into the band alignment and nature of the contact between the n-type collection layer and the perovskite, we performed hard X-ray photoelectron spectroscopy (HAXPES) measurements. In Figure 1a we present valence band spectra for TiO_2, TiO_2 modified with C_{60}-SAM (as reported previously),[20,29] and both layers with a very thin film of $CH_3NH_3PbI_3$ (sub 20 nm). We measured the binding energies of the intense core levels for all structural units of our samples as well as respective references to determine the valence band offsets following the procedure described by Kraut et al.[30] We present the XPS spectra of the Ti 2p core level and the relative binding energy shifts for the different samples in Figure S3. Using the valence band (VB) offsets and band gap values presented in Table 1, we derive the band alignment, which we show in Figure 1b. The Fermi level of the perovskite in contact with TiO_2 is very close to the conduction band minimum, a highly n-type characteristic that has been observed previously.[31,32] We and others have previously shown via both photoelectron spectroscopy and conductivity studies that metal oxides, such as TiO_2 or Al_2O_3, tend to cause electron accumulation in the perovskite material at the interface with an oxide.[31,33−35] Miller et al. have also observed that lead halide perovskites coated on p-type materials, such as poly(3,4-ethylenedioxythiophene) polystyrene sulfonate (PEDOT:PSS), exhibit a more intrinsic character.[35] Inserting a C_{60} self-assembled monolayer (SAM) between the perovskite and the TiO_2 contact shifts the perovskite valence band to lower binding energies, leading to a Fermi level more centered within the band gap and thus a more intrinsic surface. Having a different interface in the form of the C_{60}-SAM molecules with a nonpolar surface and high electron affinity could potentially cause this effect, although its exact origin is far from understood. When the perovskite film directly contacts the

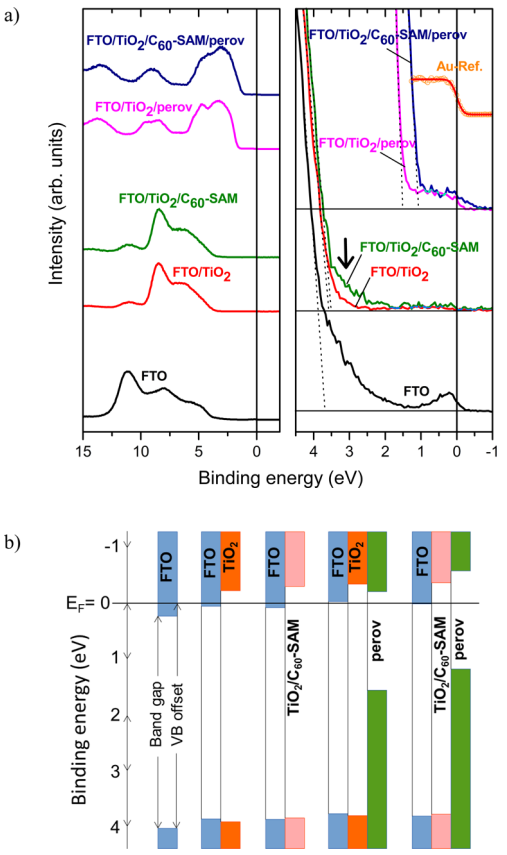

Figure 1. (a) HAXPES spectra measured with a photon energy of 8 keV for FTO (black curve), FTO/compact TiO_2 (red curve), FTO/compact TiO_2 modified with a monolayer of C_{60}-SAM (green curve), FTO/compact TiO_2/flat perovskite film (pink curve), FTO/compact TiO_2 modified with a monolayer of C_{60}-SAM/flat perovskite film (blue curve). Left panel displays the whole spectrum, right panel is a close-up on the band gap region. (b) Diagram displaying conduction and valence bands respective to the Fermi level for all measured samples.

Table 1. Valence Band Offsets Measured by HAXPES and Band Gaps of the Materials in the Samples

Sample	Band gap (eV)	VB offset (eV)
FTO	3.35	3.68
TiO_2	3.65	-
$CH_3NH_3PbI_3$	1.55	-
FTO/TiO_2	-	3.58
FTO/TiO_2/C_{60}-SAM	-	3.48
FTO/TiO_2/$CH_3NH_3PbI_3$	-	1.50
FTO/TiO_2/C_{60}-SAM/$CH_3NH_3PbI_3$	-	1.07

TiO_2, the conduction band edge of the perovskite appears to be below that of TiO_2, indicating the possibility of a barrier to electron extraction across this interface. In the sample with the C_{60}-SAM-modified TiO_2 and the perovskite, the relative shift between the vacuum levels raises the conduction band of the perovskite and removes this electronic barrier. This finding is consistent with the low efficiency of PL quenching for the perovskite coated on compact TiO_2, which is enhanced considerably with the C_{60}-SAM modification or by replacing the TiO_2 with a C_{60} film, as we show in Figure S2. We note that, although these measurements appear to indicate a favorable shift in the conduction band offsets across this heterojunction, there could also be significant changes to the

DOI: 10.1021/acs.jpclett.5b00902
J. Phys. Chem. Lett. 2015, 6, 2399−2405

surface and interface states at this junction that are not resolved here. Any changes to the interface (or surface) state density at the heterojunction are likely to have a strong influence upon the electronic properties of the subsequent device.

To characterize the performance we first constructed photovoltaic devices applying the meso-superstructured architecture (porous alumina infiltrated and capped with $CH_3NH_3PbI_{3-x}Cl_x$ perovskite), as reported previously.[2,17,36] The best PCE we achieved for cells with fullerene n-type compact layers was 13.5%, as calculated from the current−voltage scan (scan rate: 450 mV/s, scan direction: forward bias to short-circuit) and 12.7% for the steady-state measurement at the maximum power point (see Figure 2a,b). This is

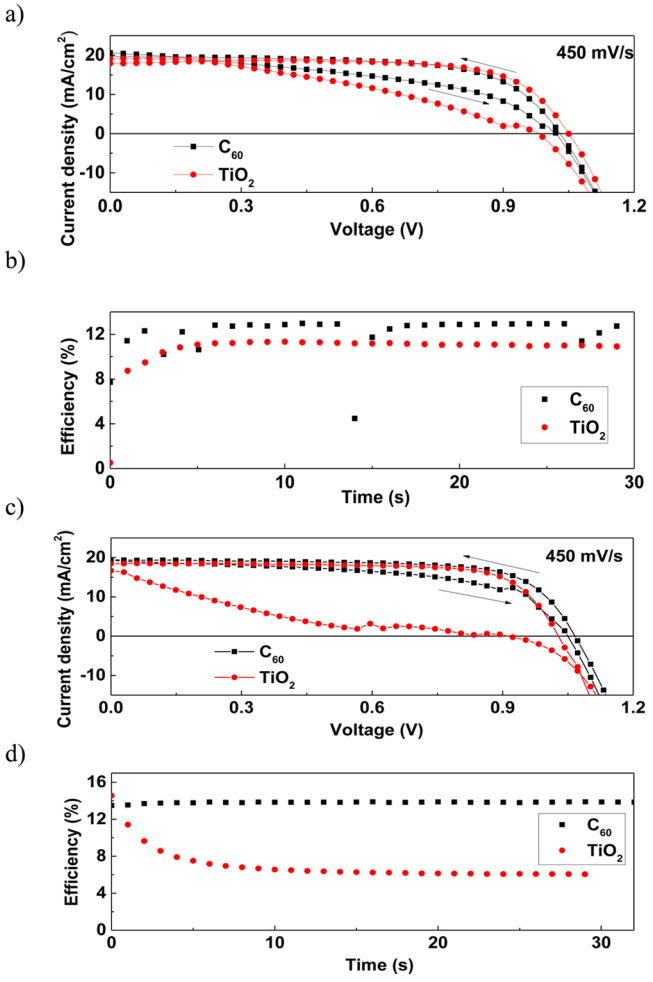

Figure 2. (a) JV curves of meso-superstructured perovskite solar cells with a C_{60} (black curve with squares) and a TiO_2 (red curve with circles) compact layer, respectively, obtained at the scanning rate of 450 mV/s and (b) stabilized power output measured close to the maximum power point of the same cells. (c) JV curves of planar heterojunction perovskite solar cells with C_{60} and TiO_2 layers, and (d) stabilized power output of the cells.

comparable to the highest JV determined efficiency of the TiO_2-based cell prepared here (13.9%), when scanned from forward-bias to short-circuit. The use of fullerene though noticeably reduces the hysteretic behavior in the JV curves and improves the stabilized PCE (10.9% for TiO_2-based cell) and the ratio of the JV-scan derived PCE to PCE measured at the maximum power point. We present the photovoltaic parameters for the forward and backward scan directions as well as the stabilized efficiencies for TiO_2 and C_{60}-based cells in Table 2.

Table 2. Photovoltaic Parameters Extracted from JV Curves Presented in Figure 2

		meso-superstructured (450 mV/s)		planar (450 mV/s)	
Compact layer		SC→FB	FB→SC	SC→FB	FB→SC
C_{60}	J_{SC} (mA/cm²)	20.6	19.8	19.4	19.6
	V_{OC} (V)	1.02	1.03	1.04	1.07
	FF	0.45	0.65	0.56	0.69
	PCE (%)	9.5	13.5	11.4	14.5
	Stab. PCE (%)	12.7		13.9	
TiO_2	J_{SC} (mA/cm²)	19.1	17.9	16.7	18.4
	V_{OC} (V)	0.98	1.05	0.92	1.04
	FF	0.37	0.70	0.14	0.72
	PCE (%)	7.1	13.9	2.1	13.6
	Stab. PCE (%)	10.9		6.1	

C_{60} is poorly soluble in dimethylformamide (DMF), the solvent used in the perovskite precursor solution, but the exposure to the solvent during spin-coating might be enough to cause partial dissolution of the fullerene film and to deteriorate the hole-blocking properties of the n-type contact. We measured the UV−vis spectra of the C_{60} films treated with different solvents to investigate their robustness to solution processing (Figure S4). There is a significant drop in the absorption band at 440 nm, which is characteristic of the fullerene absorption, upon spin-coating DMF directly on a C_{60} film. Dissolution of the compact layer is likely to strongly influence the performance and reproducibility of the manufactured devices, and will increase the hysteretic behavior in the current−voltage curves since we know that hysteresis is extremely pronounced in devices devoid of a compact layer where the perovskite makes direct contact to the transparent conducting FTO layer.[28] In order to avoid this problem, we constructed devices in planar heterojunction architecture by depositing perovskite films with a two-step vapor deposition method. We vapor deposited a PbI_2 layer directly onto the n-type compact layer (C_{60} or TiO_2) and then converted it to the perovskite structure via spin-coating methylammonium iodide (MAI) in an isopropanol solution,[37] which is a very poor solvent for the C_{60} layer. We present the photovoltaic performance (JV curves and steady-state measurements) of the champion devices in Figure 2c,d and Table 2. By following the DMF-free route we enhanced the solar cell performance and yet further reduced the hysteresis in the JV curves in conjunction with employing the fullerene compact layer. Notably, these cells are planar heterojunction devices in the "regular" configuration, which usually exhibit much more enhanced hysteresis as compared to cells incorporating mesoporous scaffolds.[23,25,28] In strong contrast, some C_{60}-based devices show negligible hysteretic behavior over a broad range of voltage scanning rates (Figure S5, Table S1). In Figure S6 we present statistics of photocurrent and efficiency extracted for a number of devices from the maximum power point measurements, for both solution-processed meso-superstructured architecture (a), and evaporated planar heterojunction architecture (b).

Since the hysteresis in the $J-V$ curves appears to be related to the electron extraction contact, we monitored the PL in

DOI: 10.1021/acs.jpclett.5b00902
J. Phys. Chem. Lett. 2015, 6, 2399−2405

reflection of the full devices at different conditions (short-circuit, forward-bias, and reverse bias) in order to see if we could directly probe changes to the electron transfer efficiency. In Figures 3a,b we present the steady state PL (monitored at

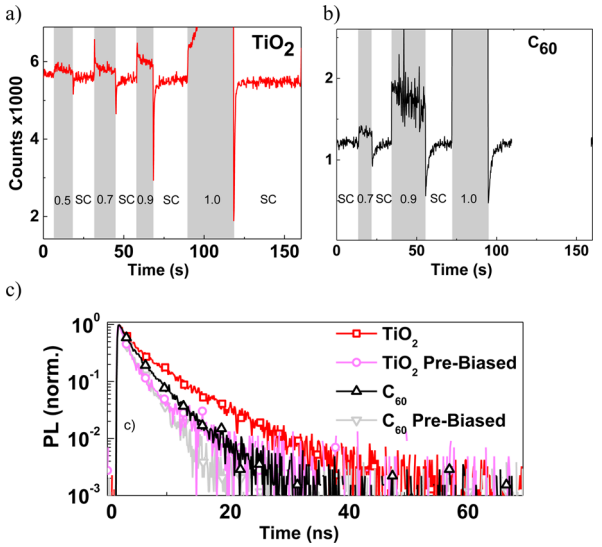

Figure 3. Steady-state PL monitored over time at the PL peak of 775 nm in working devices with (a) compact TiO_2 or (b) C_{60} acceptor layers at short-circuit and various applied forward biases. (c) The time-resolved PL decays for the devices before and immediately (within 3 s) after the application of 1 V forward bias.

the peak emission of 775 nm) of the full solar cells employing TiO_2 and C_{60} compact layers, respectively. Here, the steady-state PL, generated by recombination of free carriers within the perovskite film, is representative of the density of carriers that have not been extracted from the device; i.e., the higher the PL, the poorer the charge extraction. Applying a forward bias to the cells results in an increase in the background emission, which we assign to electroluminescence. Notably, the electroluminescence for the devices with the C_{60} compact layers is far higher than that with the TiO_2 compact layers at the same applied bias (see Figure S7a,b), suggesting improved electronic coupling between the C_{60} and perovskite conduction bands and reduced nonradiative decay at this contact under forward bias conditions. This is consistent with reports from Bolink and co-workers of efficient electroluminescence of perovskite solar cells employing C_{60}-based n-type layers.[38]

Most interestingly, we find that when the applied bias is rapidly switched from forward bias back to short-circuit, the PL is temporarily strongly quenched as compared to the situation before any biasing. This effect occurs on time scales (seconds) similar to those characteristic of the hysteresis in the JV curves.[23] It also has a clear dependence on the magnitude of the applied bias, unlike what we would expect from a ferroelectric type of response.[39,40] To further probe this effect, we performed time-resolved PL measurements on complete cells before and immediately (within 3 s) after the application of 1 V forward bias (for 20 s). We plot the results in Figure 3c, where we observe much faster PL quenching directly after forward biasing. This is consistent with the postulation that electron transfer temporarily occurs much more effectively after the application of a forward bias. However, the behavior for the TiO_2 and C_{60}-based solar cells is qualitatively different, in that the extraction in the TiO_2 based solar cell before bias is much slower than that in the C_{60}-based solar cell. As a result, the PL decay rate is only slightly increased for the C_{60}-based device, but greatly increased for the TiO_2 one. We also note that the observed decay is a convolution of hole and electron extraction, so that the extraction of electrons at the TiO_2 interface, as represented by the PL decay in Figure S2, is actually much slower than that showed in Figure 3c. After application of the electric field, the extraction rates for both samples appear to be very similar. Hence, we can conclude that solar cells employing a TiO_2 compact layer suffer from poor electron extraction, which can be temporarily improved by the application of a forward bias. We also observe that applying a reverse bias before switching back to short-circuit induces the opposite effect: reverse biasing temporarily slows the PL decay at short-circuit, which we interpret as worsening the charge extraction after reverse biasing (Figure S7c,d). The time scale of PL recovery after biasing and short-circuiting the cell is very similar to the time of current rise in steady-state measurement or the rise of electroluminescence,[20] which suggests that it is governed by the same processes.

Recently Tress et al.,[24] Xiao et al.,[27] and Zhao at al[39] independently presented data consistent with ion migration in the perovskite material being the origin of hysteretic behavior in current−voltage characterization. Under forward bias, negatively charged mobile ions (ionic species) will migrate toward the p-type charge extraction layer and mobile positive ions will migrate toward the n-type charge collection layer. Once the external field is removed (under working conditions) the displaced ions should be able to stabilize negative electronic space charge near the n-type collection layer and positive electronic space charge near the p-type collection layer, i.e., create n- and p-type doping in the perovskite layer in the regions adjacent to the appropriate charge collection layers. In reverse bias conditions, the external field will cause the ions to migrate in the opposite direction, resulting in unfavorable space charge distribution once the field is removed under working conditions (i.e., hole accumulation on the n-type collection side and electron accumulation on the p-type collection side). This is consistent with enhancing or inhibiting charge extraction dependent upon the prebiasing history. Schematic representations of band bending induced in the perovskite layer by the displaced ions and external electric field have been recently proposed.[24,28,39] We note that this concept of a polarizable p-n or p-i-n junction solar cell was first proposed by Riess in 1987, for a semiconductor with both mobile charge and ionic species,[41] and this concept has since been applied to understand the operation of light emitting electrochemical cells.[42−45] It is likely that some adaptations of these theories are still required to properly explain the origin of hysteresis in perovskite solar cells.

Assuming this picture to be largely correct, the ion migration could in effect compensate for an imperfect electronic contact between the charge collection layers and the perovskite absorber. However, for low hysteresis and high stabilized power conversion efficiency, it is clearly of vital importance for there to be a good electronic contact between perovskite and charge extraction layers and to not rely on a temporarily improved contact enabled by ion migration. The data we present in Figure 1 and 3 suggests that charge transfer from perovskite into TiO_2 in planar heterojunction architecture does not occur efficiently, and hence the large hysteresis observed in the JV curves in that system. We have shown a direct observation of the "switching" on and off of charge extraction

DOI: 10.1021/acs.jpclett.5b00902
J. Phys. Chem. Lett. 2015, 6, 2399−2405

via the prebiasing direction. Electron transfer to C_{60} occurs much more efficiently, so that the enhancements due to ion migration are only marginal, and notably under maximum power point conditions where electric field throughout the film should be low (close to flat band) the stabilized power output is high.

It is still unknown which ionic species could undergo a displacement under the applied external electric field. They could include interstitial ions and halide vacancies, whose displacement could occur on a time scale of tens of seconds.[39] Ionic motion in the material could have implications on the long-term stability of such devices, especially if the electric fields existing in the device during its operation could cause displacement of ions in the crystal lattice, which in time could result in material degradation due to regions of the film becoming increasingly nonstoichiometric.

In order to assess this possibility and compare the relative impact of TiO_2 versus C_{60} charge collection layers on device stability, we performed stability tests on larger than normal devices (meso-superstructured architecture, with 1 cm^2 active area) under simulated full spectrum AM1.5 illumination (generated from a Suntest CPS plus xenon lamp light soaking test chamber with no UV filter) at the maximum power point, and 60 °C. We have previously demonstrated that encapsulated solar cells based on mesoporous TiO_2 suffer from rapid degradation when aged under full solar irradiation, while meso-superstructured perovskite solar cells employing compact TiO_2 and mesoporous Al_2O_3 displayed greatly enhanced stability.[46] We note, however, that our previous results were obtained when aging the solar cells at open-circuit rather than under load near the maximum power point, as would be the case in real operation conditions, and at a temperature lower than 40 °C. Aging the cells under a constant load gives an indication of the real stability of the solar cell's performance. In Table 3 we

Table 3. Stabilized Photovoltaic Parameters at the Maximum Power Point of the Cells with 1 cm^2 Active Area Tested at 0.811 Sun Illumination, before 500 h of Stability Testing, with C_{60} and TiO_2 Compact Layers

	sample	Vmpp (V)	J stab. (mA/cm^2)	PCE stab. (%)
C_{60}	before aging	0.73	11.5	10.4
TiO_2	before aging	0.58	11.5	8.2

present photovoltaic parameters at a maximum power point of 1 cm^2 encapsulated cells before aging, with TiO_2 and C_{60} n-type collection layers. In Figure 4 we present our initial results of the stability study, by plotting the changes of the photovoltaic parameters measured over the period of 500 h of device operation at maximum power and elevated temperature. We recorded the JV curves every 65 min with the maximum power point voltage at which the cell is aged being reset to that determined from the latest scan. Following an initial rise, the devices based on TiO_2 compact layers exhibit a steady drop in the short-circuit photocurrent within the first 300 h (ca. 50% of the initial value), whereas the fullerene-based cells preserved over 90% of the short-circuit photocurrent in the entire time window. For these stability experiments we tested 4 or 5 devices of each configuration and aged the best cells. Although much more extensive stability testing is required to fully corroborate these results, this is an important demonstration suggesting that the fullerene-based stack can be fundamentally more stable than that incorporating compact TiO_2, and that the

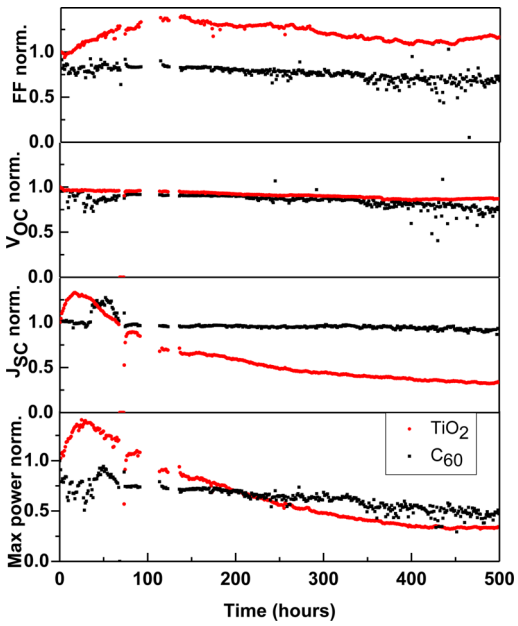

Figure 4. Evolution of normalized photovoltaic parameters extracted from JV curves measured every 65 min (from the top: fill factor, open circuit-voltage, short-circuit current), and efficiency at the maximum power point (bottom panel) of the cells with C_{60} and TiO_2 compact layer kept under load for a period of 500 h at 60 °C.

perovskite film does not lose the ability to generate photocurrent over this stressing period.

We have recently discussed the mechanism of TiO_2 instability under UV light illumination, which is responsible for photocurrent degradation in the solar cells based on mesoporous TiO_2.[46,47] We have postulated that upon TiO_2 excitation, the holes in valence band recombine with adsorbed molecular oxygen, causing its desorption and leaving positively charged deep trap sites in the TiO_2 surface. High oxygen partial pressure reduces the rate of oxygen release, but in the case of encapsulated cells, which we believe is essential for long-term protection of the perovskite from moisture, the activation of those trap sites can increase. These deep traps sites then act as sinks for electrons, with recombination of the trapped electrons occurring directly with the holes in the perovskite or hole transporter. Photocurrent degradation in TiO_2-based cells could be inhibited by application of UV-filters, but that would increase the cost of solar cell production, reduce photocurrent of the solar cell, and likely not be able to completely filter all of the absorption in the tail of the TiO_2 absorption band. The trends we present in Figure 4 for TiO_2-based cells are very similar to the ones we reported for meso-TiO_2-based devices, when aged at open-circuit condition. That might suggest that in both cases same processes govern the drop of performance in those devices. C_{60} seems to help to overcome the issue of UV instability, which is indicated by the preserved photocurrent density in the stressing period.

We note, however, that although the C_{60}-based device preserves the photocurrent very well, we observe a decline in voltage and fill factor, which is responsible for the drop of overall performance to ca. 55% of the initial value of max power. We are currently investigating further reasons for this persistent drop in voltage and fill factor, but expect imperfect layer formations and pin-holes to be largely responsible. Furthermore, here we have employed spiro-OMeTAD as the

DOI: 10.1021/acs.jpclett.5b00902
J. Phys. Chem. Lett. 2015, 6, 2399−2405

hole conductor, which we have previously shown to be nonadvantageous for enhancing the thermal stability of the perovskite. We expect further improvements in stability to be possible by replacing this with more stable hole-conductors, such as carbon nanotubes embedded in an insulating polymer matrix.[48] Before we can draw a final conclusion on C_{60}-based cells being stable, we clearly need to perform more tests and resolve the existing engineering issues, but we believe that stable photocurrent in our initial aging tests is a very encouraging observation, which points at differences in intrinsic characteristics between the employed organic and metal oxide materials.

In summary, we have shown that both solution and vapor deposited perovskite solar cells can be fabricated employing a fullerene compact layer as the bottom n-type charge extraction layer. Through spectroscopic characterization we have observed significant speeding up of the PL decay, which we interpret as improvement in the electron extraction from the photoexcited perovskite to the C_{60}, as compared to the commonly employed TiO_2 compact layer. Notably, our luminescent measurements on complete devices showed for the first time direct observation of switching on and off of charge extraction depending upon the prebiasing history. In addition to the devices displaying negligible hysteresis and high stabilized power conversion efficiency, we demonstrated stability data of the cells under operation and under full sunlight at 60 °C for 500 h. This work reveals that organic semiconductors potentially may be the ideal materials as both p- and n-type charge collection layers to achieve both high stabilized power output and long-term operational stability of perovskite solar cells.

■ ASSOCIATED CONTENT

Supporting Information

Full experimental methods, AFM and SEM images, additional XPS and UV−vis spectra, PL figures and JV curves. The Supporting Information is available free of charge on the ACS Publications website at DOI: 10.1021/acs.jpclett.5b00902.

■ AUTHOR INFORMATION

Corresponding Author

*E-mail: h.snaith1@physics.ox.ac.uk.

Funding

This work was partly funded by EPSRC and the European Union Seventh Framework Programme (FP7) through the MESO project. K.W. is funded by Oxford PV Ltd., and EPSRC DTA scholarship. A.K.-Y.J. and C.-Z.L. acknowledge the support from the Office of Naval Research (No. N00014-11-1-0300). We also acknowledge the ONR global research support.

Notes

The authors declare no competing financial interest.

■ REFERENCES

(1) NREL Best Research-Cell Efficiencies Chart. http://www.nrel.gov/ncpv/images/efficiency_chart.jpg.

(2) Lee, M. M.; Teuscher, J.; Miyasaka, T.; Murakami, T. N.; Henry, J. Efficient Hybrid Solar Cells Based on Meso-Superstructured Organometal Halide Perovskites. *Science* **2012**, *338*, 643−647.

(3) Liu, M.; Johnston, M. B.; Snaith, H. J. Efficient Planar Heterojunction Perovskite Solar Cells by Vapour Deposition. *Nature* **2013**, *501*, 395−398.

(4) Burschka, J.; Pellet, N.; Moon, S.-J.; Humphry-Baker, R.; Gao, P.; Nazeeruddin, M. K.; Grätzel, M. Sequential Deposition as a Route to High-Performance Perovskite-Sensitized Solar Cells. *Nature* **2013**, *499*, 316−319.

(5) Zhou, H.; Chen, Q.; Li, G.; Luo, S.; Song, T. -b.; Duan, H.-S.; Hong, Z.; You, J.; Liu, Y.; Yang, Y. Interface Engineering of Highly Efficient Perovskite Solar Cells. *Science* **2014**, *345*, 542−546.

(6) Jeon, N. J.; Noh, J. H.; Yang, W. S.; Kim, Y. C.; Ryu, S.; Seo, J.; Seok, S. Il. Compositional Engineering of Perovskite Materials for High-Performance Solar Cells. *Nature* **2015**, *517*, 476−480.

(7) Green, M. A.; Ho-Baillie, A.; Snaith, H. J. The Emergence of Perovskite Solar Cells. *Nat. Photonics* **2014**, *8*, 506−514.

(8) Jung, H. S.; Park, N.-G. Perovskite Solar Cells: From Materials to Devices. *Small* **2014**, *11*, 10−25.

(9) Tan, Z.-K.; Moghaddam, R. S.; Lai, M. L.; Docampo, P.; Higler, R.; Deschler, F.; Price, M.; Sadhanala, A.; Pazos, L. M.; Credgington, D.; et al. Bright Light-Emitting Diodes Based on Organometal Halide Perovskite. *Nat. Nanotechnol.* **2014**, *9*, 687−692.

(10) Li, Y.; Zhang, D.-Q.; Duan, L.; Zhang, R.; Wang, L.-D.; Qiu, Y. Elucidation of the Electron Injection Mechanism of Evaporated Cesium Carbonate Cathode Interlayer for Organic Light-Emitting Diodes. *Appl. Phys. Lett.* **2007**, *90*, 012119.

(11) Kim, Y.-H.; Cho, H.; Heo, J. H.; Kim, T.-S.; Myoung, N.; Lee, C.-L.; Im, S. H.; Lee, T.-W. Multicolored Organic/Inorganic Hybrid Perovskite Light-Emitting Diodes. *Adv. Mater.* **2014**, *27*, 1248−1254.

(12) Jung, J. W.; Williams, S. T.; Jen, A. K.-Y. Low-Temperature Processed High-Performance Flexible Perovskite Solar Cells via Rationally Optimized Solvent Washing Treatment. *RSC Adv.* **2014**, *4*, 62971−62977.

(13) Deschler, F.; Price, M.; Pathak, S.; Klintberg, L. E.; Jarausch, D.; Higler, R.; Hu, S.; Leijtens, T.; Stranks, S. D.; Snaith, H. J.; et al. High Photoluminescence Efficiency and Optically Pumped Lasing in Solution-Processed Mixed Halide Perovskite Semiconductors. *J. Phys. Chem. Lett.* **2014**, *5*, 1421−1426.

(14) Sutherland, B. R.; Hoogland, S.; Adachi, M. M.; Wong, C. T. O.; Sargent, E. H.; Al, S. E. T. Conformal Organohalide Perovskites Enable Lasing on Spherical Resonators. *ACS Nano* **2014**, *8*, 10947−10952.

(15) Horváth, E.; Spina, M.; Szekrényes, Z.; Kamarás, K.; Gaal, R.; Gachet, D.; Forró, L. Nanowires of Methylammonium Lead Iodide ($CH_3NH_3PbI_3$) Prepared by Low Temperature Solution-Mediated Crystallization. *Nano Lett.* **2014**, *14*, 6761−6766.

(16) Moehl, T.; Im, J. H.; Lee, Y. H.; Domanski, K.; Giordano, F.; Zakeeruddin, S. M.; Dar, M. I.; Heiniger, L.; Nazeeruddin, M. K.; Park, N.; et al. Strong Photocurrent Amplification in Perovskite Solar Cells with a Porous TiO_2 Blocking Layer under Reverse Bias. *J. Phys. Chem. Lett.* **2014**, *5*, 3931−3936.

(17) Wojciechowski, K.; Saliba, M.; Leijtens, T.; Abate, A.; Snaith, H. J. Sub-150 °C Processed Meso-Superstructured Perovskite Solar Cells with Enhanced Efficiency. *Energy Environ. Sci.* **2014**, *7*, 1142.

(18) Liu, D.; Kelly, T. L. Perovskite Solar Cells with a Planar Heterojunction Structure Prepared Using Room-Temperature Solution Processing Techniques. *Nat. Photonics* **2014**, *8*, 133−138.

(19) Noel, N. K.; Abate, A.; Stranks, S. D.; Parrott, E. S.; Burlakov, V. M.; Goriely, A.; Snaith, H. J. Enhanced Photoluminescence and Solar Cell Performance via Lewis Base Passivation of Organic−Inorganic Lead Halide Perovskites. *ACS Nano* **2014**, *8*, 9815−9821.

(20) Wojciechowski, K.; Stranks, S. D.; Abate, A.; Sadoughi, G.; Sadhanala, A.; Kopidakis, N.; Rumbles, G.; Li, C.; Friend, R. H.; Jen, A. K.; et al. Heterojunction Modification for Highly Efficient Organic−Inorganic Perovskite Solar Cells. *ACS Nano* **2014**, *8*, 12701−12709.

(21) Zhang, Q.; Park, K.; Xi, J.; Myers, D.; Cao, G. Recent Progress in Dye-Sensitized Solar Cells Using Nanocrystallite Aggregates. *Adv. Energy Mater.* **2011**, *1*, 988−1001.

(22) Shi, J.; Xu, X.; Li, D.; Meng, Q. Interfaces in Perovskite Solar Cells. *Small* **2015**, DOI: 10.1002/smll.201403534.

(23) Snaith, H. J.; Abate, A.; Ball, J. M.; Eperon, G. E.; Leijtens, T.; Noel, N. K.; Stranks, S. D.; Wang, J. T.; Wojciechowski, K.; Zhang, W.

DOI: 10.1021/acs.jpclett.5b00902
J. Phys. Chem. Lett. 2015, 6, 2399−2405

Anomalous Hysteresis in Perovskite Solar Cells. *J. Phys. Chem. Lett.* **2014**, *17*, 1511−1515.
(24) Tress, W.; Marinova, N.; Moehl, T.; Zakeeruddin, S. M.; Mohammad, K. N.; Grätzel, M. Understanding the Rate-Dependent J-V Hysteresis, Slow Time Component, and Aging in $CH_3NH_3PbI_3$ Perovskite Solar Cells: The Role of a Compensated Electric Field. *Energy Environ. Sci.* **2015**, *8*, 995−1004.
(25) Unger, E. L.; Hoke, E. T.; Bailie, C. D.; Nguyen, W. H.; Bowring, A. R.; Heumuller, T.; Christoforo, M. G.; McGehee, M. D. Hysteresis and Transient Behavior in Current−Voltage Measurements of Hybrid-Perovskite Absorber Solar Cells. *Energy Environ. Sci.* **2014**, *7*, 3690−3698.
(26) Liu, S.; Zheng, F.; Koocher, N. Z.; Takenaka, H.; Wang, F.; Rappe, A. M. Ferroelectric Domain Wall Induced Band-Gap Reduction and Charge Separation in Organometal Halide Perovskites. *J. Phys. Chem. Lett.* **2015**, *6*, 693−699.
(27) Xiao, Z.; Yuan, Y.; Shao, Y.; Wang, Q.; Dong, Q.; Bi, C.; Sharma, P.; Gruverman, A.; Huang, J. Giant Switchable Photovoltaic Effect in Organometal Trihalide Perovskite Devices. *Nat. Mater.* **2014**, *14*, 193−198.
(28) Zhang, Y.; Liu, M.; Eperon, G. E.; Leijtens, T.; McMeekin, D. P.; Saliba, M.; Zhang, W.; De Bastiani, M.; Petrozza, A.; Herz, L.; et al. Charge Selective Contacts, Mobile Ions and Anomalous Hysteresis in Organic−Inorganic Perovskite Solar Cells. *Mater. Horiz.* **2015**, *2*, 315−322.
(29) Abrusci, A.; Stranks, S. D.; Docampo, P.; Yip, H.-L.; Jen, A. K.-Y.; Snaith, H. J. High Performance Perovskite−Polymer Hybrid Solar Cells via Electronic Coupling with Fullerene Monolayers. *Nano Lett.* **2013**, *13*, 3124−3128.
(30) Kraut, E.; Grant, R.; Waldrop, J.; Kowalczyk, S. Precise Determination of the Valence-Band Edge in X-Ray Photoemission Spectra: Application to Measurement of Semiconductor Interface Potentials. *Phys. Rev. Lett.* **1980**, *44*, 1620−1623.
(31) Leijtens, T.; Stranks, S. D.; Eperon, G. E.; Lindblad, R.; Johansson, E. M. J.; McPherson, I. J.; Rensmo, H.; Ball, J. M.; Lee, M. M.; Snaith, H. J. Electronic Properties of Meso-Superstructured and Planar Organometal Halide Perovskite Films: Charge Trapping, Photodoping, and Carrier Mobility. *ACS Nano* **2014**, *8*, 7147−7155.
(32) Edri, E.; Kirmayer, S.; Mukhopadhyay, S.; Gartsman, K.; Hodes, G.; Cahen, D. Elucidating the Charge Carrier Separation and Working Mechanism of $CH_3NH_3PbI_{3-x}Cl_x$ Perovskite Solar Cells. *Nat. Commun.* **2014**, *5*, 1−8.
(33) Lindblad, R.; Bi, D.; Park, B.; Oscarsson, J.; Gorgoi, M.; Siegbahn, H.; Odelius, M.; Johansson, E. M. J.; Rensmo, H. Electronic Structure of $TiO_2/CH_3NH_3PbI_3$ Perovskite Solar Cell Interfaces. *J. Phys. Chem. Lett.* **2014**, *5*, 648−653.
(34) Schulz, P.; Edri, E.; Kirmayer, S.; Hodes, G.; Cahen, D.; Kahn, A. Interface Energetics in Organo-Metal Halide Perovskite-Based Photovoltaic Cells. *Energy Environ. Sci.* **2014**, *7*, 1377−1384.
(35) Miller, E. M.; Zhao, Y.; Mercado, C.; Saha, S.; Luther, J. M.; Zhu, K.; Stevanovic, V.; Perkins, C. L.; van de Lagemaat, J. Substrate-Controlled Band Positions in $CH_3NH_3PbI_3$ Perovskite Films. *Phys. Chem. Chem. Phys.* **2014**, *16*, 22122−22130.
(36) Ball, J. M.; Lee, M. M.; Hey, A.; Snaith, H. J. Low-Temperature Processed Meso-Superstructured To Thin-Film Perovskite Solar Cells. *Energy Environ. Sci.* **2013**, *6*, 1739.
(37) Xiao, Z.; Bi, C.; Shao, Y.; Dong, Q.; Wang, Q.; Yuan, Y.; Wang, C.; Gao, Y.; Huang, J. Efficient, High Yield Perovskite Photovoltaic Devices Grown by Interdiffusion of Solution-Processed Precursor Stacking Layers. *Energy Environ. Sci.* **2014**, *7*, 2619−2623.
(38) Gil-Escrig, L.; Longo, G.; Pertegás, A.; Roldan, C.; Soriano Portillo, A.; Sessolo, M.; Bolink, H. J. Efficient Photovoltaic and Electroluminescent Perovskite Devices. *Chem. Commun.* **2014**, *1*, 569−571.
(39) Zhao, Y.; Liang, C.; Zhang, H. M.; Li, D.; Tian, D.; Li, G.; Jing, X.; Zhang, W.; Xiao, W.; Liu, Q.; et al. Anomalously Large Interface Charge in Polarity-Switchable Photovoltaic Devices: An Indication of Mobile Ions in Organic−Inorganic Halide Perovskites. *Energy Environ. Sci.* **2015**, *8*, 1256−1260.
(40) Merz, W. J. Switching Time in Ferroelectric $BaTiO_3$ and Its Dependence on Crystal Thickness. *J. Appl. Phys.* **1956**, *27*, 938.
(41) Riess, I. Voltage-Controlled Structure of Certain P−N and P−I−N Junctions. *Phys. Rev. B* **1987**, *35*, 5740.
(42) Riess, I.; Cahen, D. Introduction, I. Analysis of Light Emitting Polymer Electrochemical Cells. *J. Appl. Phys.* **1997**, *82*, 3147−3151.
(43) Pei, Q.; Yu, G.; Zhang, C.; Yang, Y.; Heeger, A. J. Polymer Light-Emitting Electrochemical Cells. *Science* **1995**, *269*, 1086−1088.
(44) Pei, Q.; Yang, Y.; Yu, G.; Zhang, C.; Heeger, A. J. Polymer Light-Emitting Electrochemical Cells: In Situ Formation of a Light-Emitting p−n Junction. *J. Am. Chem. Soc.* **1996**, *118*, 3922−3929.
(45) Edman, L. Bringing Light to Solid-State Electrolytes: The Polymer Light-Emitting Electrochemical Cell. *Electrochim. Acta* **2005**, *50*, 3878−3885.
(46) Leijtens, T.; Eperon, G. E.; Pathak, S.; Abate, A.; Lee, M. M.; Snaith, H. J. Overcoming Ultraviolet Light Instability of Sensitized TiO_2 with Meso-Superstructured Organometal Tri-Halide Perovskite Solar Cells. *Nat. Commun.* **2013**, *4*, 2885.
(47) Pathak, S. K.; Abate, A.; Ruckdeschel, P.; Roose, B.; Gödel, K. C.; Vaynzof, Y.; Santhala, A.; Watanabe, S.-I.; Hollman, D. J.; Noel, N.; et al. Performance and Stability Enhancement of Dye-Sensitized and Perovskite Solar Cells by Al Doping of TiO_2. *Adv. Funct. Mater.* **2014**, *24*, 6046−6055.
(48) Habisreutinger, S. N.; Leijtens, T.; Eperon, G. E.; Stranks, S. D.; Nicholas, R. J.; Snaith, H. J. Carbon Nanotube/Polymer Composites as a Highly Stable Hole Collection Layer in Perovskite Solar Cells. *Nano Lett.* **2014**, *14*, 5561−5568.

DOI: 10.1021/acs.jpclett.5b00902
J. Phys. Chem. Lett. 2015, 6, 2399−2405